Jets Lecture 4

Tuomas Savolainen
Max-Planck-Institut für Radioastronomie, Bonn, Germany

tsavolainen@mpifr.de

Autumn 2011

Outline

Relativistic effects summary

Observations of a relativistic jet having a Lorentz factor Γ and an angle to los θ, are affected by the following transformations (see Rybicki & Lightman Ch.4):

Relativistic effects summary

Observations of a relativistic jet having a Lorentz factor Γ and an angle to los θ, are affected by the following transformations (see Rybicki & Lightman Ch.4):

- *Doppler shift* $\nu = \delta\nu'$, where $\delta = \Gamma^{-1}(1 - \beta\cos\theta)^{-1}$ is the *relativistic Doppler factor*

Relativistic effects summary

Observations of a relativistic jet having a Lorentz factor Γ and an angle to los θ, are affected by the following transformations (see Rybicki & Lightman Ch.4):

- *Doppler shift* $\nu = \delta\nu'$, where $\delta = \Gamma^{-1}(1 - \beta\cos\theta)^{-1}$ is the *relativistic Doppler factor*
- *Compression* of time scales $\Delta t = \delta^{-1}\Delta t'$

Relativistic effects summary

Observations of a relativistic jet having a Lorentz factor Γ and an angle to los θ, are affected by the following transformations (see Rybicki & Lightman Ch.4):

- *Doppler shift* $\nu = \delta\nu'$, where $\delta = \Gamma^{-1}(1 - \beta\cos\theta)^{-1}$ is the *relativistic Doppler factor*
- *Compression* of time scales $\Delta t = \delta^{-1}\Delta t'$
- *Relativistic aberration* of light $\sin\theta = \frac{\sin\theta'}{\Gamma(1+\beta\cos\theta')}$; $\cos\theta = \frac{\cos\theta'+\beta}{1+\beta\cos\theta'}$, which leads to *relativistic beaming*, i.e., isotropic emission in the rest frame appears beamed in the observer's frame

Relativistic effects summary

- *Doppler boosting* of emitted flux density from a discrete source $F(\nu) = \delta^{3-\alpha} F'(\nu)$, where α is the power-law spectral index ($F(\nu) \propto \nu^{\alpha}$)

Relativistic effects summary

- *Doppler boosting* of emitted flux density from a discrete source $F(\nu) = \delta^{3-\alpha} F'(\nu)$, where α is the power-law spectral index ($F(\nu) \propto \nu^{\alpha}$)
- *Doppler boosting* of emitted flux density from a continuous jet $F(\nu) = \frac{\delta^{2-\alpha}}{\Gamma} F'(\nu)$

Relativistic effects summary

- *Doppler boosting* of emitted flux density from a discrete source $F(\nu) = \delta^{3-\alpha} F'(\nu)$, where α is the power-law spectral index ($F(\nu) \propto \nu^{\alpha}$)
- *Doppler boosting* of emitted flux density from a continuous jet $F(\nu) = \frac{\delta^{2-\alpha}}{\Gamma} F'(\nu)$
- Increase of brightness temperature: $T_{\rm B} = \delta T'_{\rm B}$

Relativistic effects summary

- *Doppler boosting* of emitted flux density from a discrete source $F(\nu) = \delta^{3-\alpha} F'(\nu)$, where α is the power-law spectral index ($F(\nu) \propto \nu^{\alpha}$)
- *Doppler boosting* of emitted flux density from a continuous jet $F(\nu) = \frac{\delta^{2-\alpha}}{\Gamma} F'(\nu)$
- Increase of brightness temperature: $T_{\mathrm{B}} = \delta T'_{\mathrm{B}}$
- *Apparent superluminal motion* $\beta_{\mathrm{app}} = \frac{\beta \sin\theta}{1-\beta\cos\theta}$

Radiative processes: Synchrotron emission continued (see Rybicki & Lightman Ch. 6)

Recap from the previous lecture - Synchrotron power

(Notice that Γ refers to Lorentz factor of the bulk flow and γ refers to Lorentz factor of particles.)

- Moving electron in B-field experiences acceleration due to Lorentz-force and radiates:
  - $v << c$, cyclotron emission at $\nu_\mathrm{L} = \frac{eB}{2\pi mc}$
  - $v \sim c$, synchrotron emission
- Relativistic beaming changes the total emitted power and spectrum of synchrotron radiation compared to non-relativistic case
- Total emitted power $P = \frac{2e^4\gamma^2B^2v^2\sin^2\Phi}{3c^5m^2}$, and averaged over pitch-angle Φ, $\langle P\rangle = 4/3\sigma_T c\beta^2\gamma^2 U_B$, where σ_T is Thomson cross-section and $U_B = B^2/(8\pi)$

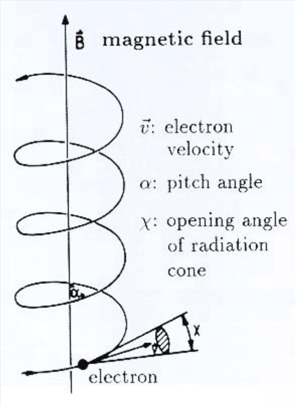

Courtesy of M.Dahlem

Recap from the previous lecture - Synchrotron lifetime

- Power radiated (and energy lost): $-\frac{dE}{dt} = \frac{4e^4 B^2 E^2}{9m^4 c^7}$

Recap from the previous lecture - Synchrotron lifetime

- Power radiated (and energy lost): $-\frac{dE}{dt} = \frac{4e^4 B^2 E^2}{9m^4 c^7}$
  - depends on the second power of particle energy and magnetic flux density

Recap from the previous lecture - Synchrotron lifetime

- Power radiated (and energy lost): $-\frac{dE}{dt} = \frac{4e^4 B^2 E^2}{9m^4 c^7}$
  - depends on the second power of particle energy and magnetic flux density
  - inversely proportional to the 4th power of particle mass

Recap from the previous lecture - Synchrotron lifetime

- Power radiated (and energy lost): $-\frac{dE}{dt} = \frac{4e^4 B^2 E^2}{9m^4 c^7}$
  - depends on the second power of particle energy and magnetic flux density
  - inversely proportional to the 4th power of particle mass
- Integrating gives $E(t) = \frac{E_0}{1+kE_0 t}$ from which half-life of an electron with initial energy γ_0 is $t_{1/2} = \frac{5\times10^8}{\gamma_0 B^2}$ seconds

Recap from the previous lecture - Single-electron spectrum

Courtesy of TU Dortmund

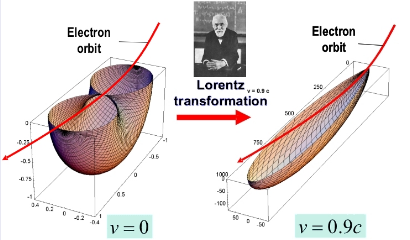

Relativistic beaming → only short pulses of emission seen by an observer → spectrum spreads

Courtesy of C. Flynn

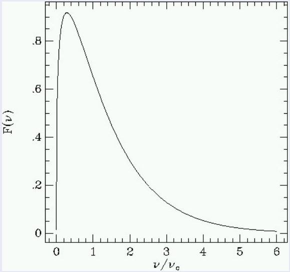

$P(\nu) = \frac{\sqrt{3}e^3 B \sin\Phi}{mc^2} \frac{\nu}{\nu_c} \int_{\nu/\nu_c}^{\infty} K_{5/3}(\xi) d\xi$

where $\nu_c = 3/2\gamma^2 \nu_L \sin\Phi$. Spectrum peaks at $\nu \approx 0.29\nu_c$

Recap from the previous lecture - Ensemble of electrons

- Consider power-law electron energy distribution (expected from cosmic accelerators): $n(\gamma)d\gamma = n_0\gamma^{-p}d\gamma$

Recap from the previous lecture - Ensemble of electrons

- Consider power-law electron energy distribution (expected from cosmic accelerators): $n(\gamma)d\gamma = n_0\gamma^{-p}d\gamma$
- The spectrum is given by integrating $P_\nu^{tot} = \int_1^\infty P_\nu(\gamma)n(\gamma)d\gamma$ This is hard to do analytically (but can be done). An easy way is to approximate the single-eletron spectrum with a δ-function: $P_\nu(\gamma) \approx 4/3\beta^2\gamma^2 c\sigma_T U_B \delta(\nu - \gamma^2\nu_L)$.

Recap from the previous lecture - Ensemble of electrons

- Consider power-law electron energy distribution (expected from cosmic accelerators): $n(\gamma)d\gamma = n_0\gamma^{-p}d\gamma$
- The spectrum is given by integrating $P_\nu^{tot} = \int_1^\infty P_\nu(\gamma)n(\gamma)d\gamma$ This is hard to do analytically (but can be done). An easy way is to approximate the single-eletron spectrum with a δ-function: $P_\nu(\gamma) \approx 4/3\beta^2\gamma^2 c\sigma_T U_B \delta(\nu - \gamma^2\nu_L)$.
- The resulting spectrum (averaged over pitch angles) is $P_\nu^{tot} = \frac{2}{3}c\sigma_T n_0 \frac{U_B}{\nu_L}\left(\frac{\nu}{\nu_L}\right)^{-\frac{p-1}{2}}$. → Power-law electron energy spectrum produces a power-law synchrotron spectrum! (Between $\gamma_{min}^2\nu_L < \nu < \gamma_{max}^2\nu_L$, not taking low-frequency self-absorption into account.) Spectral index is connected to the power-law index of underlying electron distribution.

Exact synchrotron emission formulae

- Exact analytical solution for synchrotron intensity from a power-law electron energy distribution with $N_0(\vec{k})$ being the normalization factor for number of electrons along the l.o.s. moving towards the observer:
  $I_\nu^{tot} = \frac{\sqrt{3}}{p+1}\Gamma\left(\frac{3p-1}{12}\right)\Gamma\left(\frac{3p+19}{12}\right)\frac{e^2}{mc^2}\left(\frac{3e}{2\pi m^3 c^5}\right)^{(p-1)/2}$
  $\times N_0(\vec{k})(B\sin\Phi)^{(p+1)/2}\nu^{-(p-1)/2}$

Exact synchrotron emission formulae

- Exact analytical solution for synchrotron intensity from a power-law electron energy distribution with $N_0(\vec{k})$ being the normalization factor for number of electrons along the l.o.s. moving towards the observer:
$$I_\nu^{tot} = \frac{\sqrt{3}}{p+1}\Gamma\left(\frac{3p-1}{12}\right)\Gamma\left(\frac{3p+19}{12}\right)\frac{e^2}{mc^2}\left(\frac{3e}{2\pi m^3 c^5}\right)^{(p-1)/2} \times N_0(\vec{k})(B\sin\Phi)^{(p+1)/2}\nu^{-(p-1)/2}$$
- ...and for emission along a path length L [cm] through a homogeneous and isotropic electron distribution of number density $nd\gamma = n_0\gamma^{-p}d\gamma$ averaged over random field directions:
$$I_\nu^{tot} = a(p)\frac{e^3}{mc^2}\left(\frac{3e}{4\pi m^3 c^5}\right)^{(p-1)/2} n_0 L B^{(p+1)/2}\nu^{-(p-1)/2}$$
$$= 13.5a(p)n_0 L B^{(p+1)/2}\left(\frac{6.26\times 10^{18}}{\nu}\right)^{(p-1)/2} \quad [\mathrm{Jy\ steradian}^{-1}],$$
where $a(p)$ is a product of multiple Γ-functions and varies slowly between 0.28 and 0.08 as p varies between 1 and 5.

Synchrotron self-absorption

- To every emission process there is a corresponding absorption process. In case of synchrotron emission, this is called *synchrotron self-absorption*
- At low frequencies, the power-law spectrum turns over as the opacity to synchrotron self-absorption increases
- For $\tau >> 1$, $I_\nu \propto \nu^{5/2} B^{-1/2}$ (this holds for a homogeneous synchrotron source – if there are gradients in B or n_0 across the source, the slope is flatter than 5/2)

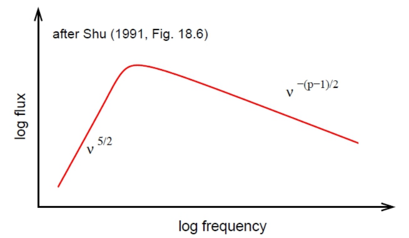

Turnover frequency ν_m is close to $\nu(\tau = 1)$ but it is not exactly that.

Polarization of synchrotron emission

- Synchrotron radiation is partially linearly polarized and it can be characterized by its powers per unit frequency $P_{||}(\nu)$ and $P_{\perp}(\nu)$ in directions parallel and perpendicular to the B-field projection on the sky
- Degree of linear polarization is $\Pi(\nu) = \frac{P_{\perp}(\nu) - P_{||}(\nu)}{P_{\perp}(\nu) - P_{||}(\nu)} = \frac{G(x)}{F(x)}$, where $G(x) = xK_{2/3}$ and $F(x) = x\int_x^{\infty} K_{5/3}(\xi)d\xi$
- Degree of linear polarization is high: 75% for frequency-integrated radiation!

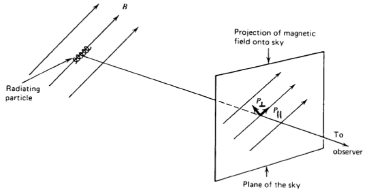

(Rybicki & Lightman, 1979, Fig. 6.7)

For an optically thin synchtron emission, the polarization vector lies perpendicular to projected B-field orientation. Polarization is a great tool for studying the magnetic field!

Polarization of synchrotron emission

- For a power-law electron energy distripution $\Pi = \frac{p+1}{p+\frac{7}{3}}$ in the optically thin part of the spectrum
- For $p = 2.5$, $\Pi \approx 70\%$. Very high!
- In real synchrotron sources Π is typically lower than this. This can be due to magnetic field inhomogeneities or due to Faraday-depolarization
- For $\tau >> 1$, Π is significantly smaller compared to optically thin case and the electric vector is parallel to projected B-field $\rightarrow$ 90 deg flip in EVPA when going from optically thick to optically thin

Applications of synchrotron theory to astrophysical jets

Recognizing a synchrotron source

Astrophysical source of synchrotron radiation has

- Non-thermal radio(-optical/X-ray) spectrum
- Typically high degree of linear polarization and low degree of circular polarization ($\sim 1/\gamma(\nu)$)
- Typically high T_B

What can we learn about the physics of the jets based on the synchrotron emission properties?

- At least there must by highly relativistic electrons and magnetic fields present in the jet. Can we go beyond this simple fact?

Measuring B and n_0 in self-absorbed synchrotron sources

- The flux from a source at frequencies where $\tau >> 1$ becomes $F_\nu = \pi S_\nu a^2 \propto \frac{\nu^{5/2}\Theta^2}{B^{1/2}}$, where Θ is the angular extent of the source

Measuring B and n_0 in self-absorbed synchrotron sources

- The flux from a source at frequencies where $\tau >> 1$ becomes $F_\nu = \pi S_\nu a^2 \propto \frac{\nu^{5/2}\Theta^2}{B^{1/2}}$, where Θ is the angular extent of the source
- The above is approximately true also at the spectral turnover, which gives a possibility to calculate B, n_0 and electron energy density U_{re} if S_m in Jy, ν_m in GHz, and Θ_m in mas are measured to high enough accuracy:
  $B = 10^{-5} b(\alpha)\Theta(\nu_\mathrm{m})^4 \nu_\mathrm{m}^5 S_\mathrm{m}^{-2} \frac{\delta}{1+z} \quad [\mathrm{G}]$
  $n_0 = n(\alpha) D_\mathrm{Gpc}^{-1} \Theta(\nu_\mathrm{m})^{-(7-4\alpha)} \nu_\mathrm{m}^{-(5-4\alpha)} S_\mathrm{m}^{3-2\alpha}$
  $\times (1+z)^{2(3-\alpha)} \delta^{-2(2-\alpha)} \quad [\mathrm{erg}^{-2\alpha}\,\mathrm{cm}^{-3}]$
  $U_\mathrm{re} \approx f(\alpha, \nu_2/\nu_1) D_\mathrm{Gpc}^{-1} \Theta(\nu_\mathrm{m})^{-9} \nu_\mathrm{m}^{-7} S_\mathrm{m}^4 (1+z)^7 \delta^{-5} \quad [\mathrm{erg\,cm}^{-3}]$
  (see *Marscher 1983 ApJ 264, 296* for tabulated values of b and n)

Measuring B and n_0 in self-absorbed synchrotron sources

- The flux from a source at frequencies where $\tau >> 1$ becomes $F_\nu = \pi S_\nu a^2 \propto \frac{\nu^{5/2}\Theta^2}{B^{1/2}}$, where Θ is the angular extent of the source
- The above is approximately true also at the spectral turnover, which gives a possibility to calculate B, n_0 and electron energy density U_{re} if S_m in Jy, ν_m in GHz, and Θ_m in mas are measured to high enough accuracy:
$$B = 10^{-5} b(\alpha)\Theta(\nu_\mathrm{m})^4 \nu_\mathrm{m}^5 S_\mathrm{m}^{-2} \frac{\delta}{1+z} \quad [\mathrm{G}]$$
$$n_0 = n(\alpha) D_\mathrm{Gpc}^{-1} \Theta(\nu_\mathrm{m})^{-(7-4\alpha)} \nu_\mathrm{m}^{-(5-4\alpha)} S_\mathrm{m}^{3-2\alpha} \times (1+z)^{2(3-\alpha)} \delta^{-2(2-\alpha)} \quad [\mathrm{erg}^{-2\alpha}\,\mathrm{cm}^{-3}]$$
$$U_\mathrm{re} \approx f(\alpha, \nu_2/\nu_1) D_\mathrm{Gpc}^{-1} \Theta(\nu_\mathrm{m})^{-9} \nu_\mathrm{m}^{-7} S_\mathrm{m}^4 (1+z)^7 \delta^{-5} \quad [\mathrm{erg\,cm}^{-3}]$$
(see *Marscher 1983 ApJ 264, 296* for tabulated values of b and n)
- Above formulae assume a homogeneous synchrotron source with random B-field orientations.

Measuring B and n_0 in self-absorbed synchrotron sources

- The flux from a source at frequencies where $\tau >> 1$ becomes $F_\nu = \pi S_\nu a^2 \propto \frac{\nu^{5/2}\Theta^2}{B^{1/2}}$, where Θ is the angular extent of the source
- The above is approximately true also at the spectral turnover, which gives a possibility to calculate B, n_0 and electron energy density U_{re} if S_m in Jy, ν_m in GHz, and Θ_m in mas are measured to high enough accuracy:
  $B = 10^{-5} b(\alpha)\Theta(\nu_\mathrm{m})^4 \nu_\mathrm{m}^5 S_\mathrm{m}^{-2} \frac{\delta}{1+z} \quad [\mathrm{G}]$
  $n_0 = n(\alpha) D_\mathrm{Gpc}^{-1} \Theta(\nu_\mathrm{m})^{-(7-4\alpha)} \nu_\mathrm{m}^{-(5-4\alpha)} S_\mathrm{m}^{3-2\alpha}$
  $\quad \times (1+z)^{2(3-\alpha)} \delta^{-2(2-\alpha)} \quad [\mathrm{erg}^{-2\alpha}\,\mathrm{cm}^{-3}]$
  $U_\mathrm{re} \approx f(\alpha, \nu_2/\nu_1) D_\mathrm{Gpc}^{-1} \Theta(\nu_\mathrm{m})^{-9} \nu_\mathrm{m}^{-7} S_\mathrm{m}^4 (1+z)^7 \delta^{-5} \quad [\mathrm{erg\,cm}^{-3}]$
  (see *Marscher 1983 ApJ 264, 296* for tabulated values of b and n)
- Above formulae assume a homogeneous synchrotron source with random B-field orientations.
- Can be used to measure B-fields in compact jets and in mini-lobes of young radio sources.

Measuring B and n_0 in self-absorbed synchrotron sources

- The flux from a source at frequencies where $\tau >> 1$ becomes $F_\nu = \pi S_\nu a^2 \propto \frac{\nu^{5/2}\Theta^2}{B^{1/2}}$, where Θ is the angular extent of the source
- The above is approximately true also at the spectral turnover, which gives a possibility to calculate B, n_0 and electron energy density U_{re} if S_m in Jy, ν_m in GHz, and Θ_m in mas are measured to high enough accuracy:
  $B = 10^{-5} b(\alpha)\Theta(\nu_\mathrm{m})^4 \nu_\mathrm{m}^5 S_\mathrm{m}^{-2} \frac{\delta}{1+z} \quad [\mathrm{G}]$
  $n_0 = n(\alpha) D_\mathrm{Gpc}^{-1} \Theta(\nu_\mathrm{m})^{-(7-4\alpha)} \nu_\mathrm{m}^{-(5-4\alpha)} S_\mathrm{m}^{3-2\alpha}$
  $\times (1+z)^{2(3-\alpha)} \delta^{-2(2-\alpha)} \quad [\mathrm{erg}^{-2\alpha}\,\mathrm{cm}^{-3}]$
  $U_\mathrm{re} \approx f(\alpha, \nu_2/\nu_1) D_\mathrm{Gpc}^{-1} \Theta(\nu_\mathrm{m})^{-9} \nu_\mathrm{m}^{-7} S_\mathrm{m}^4 (1+z)^7 \delta^{-5} \quad [\mathrm{erg\,cm}^{-3}]$
  (see *Marscher 1983 ApJ 264, 296* for tabulated values of b and n)
- Above formulae assume a homogeneous synchrotron source with random B-field orientations.
- Can be used to measure B-fields in compact jets and in mini-lobes of young radio sources.
- Requires very challenging multi-frequency VLBI observations.

Example: VLBA spectra of 3C 273

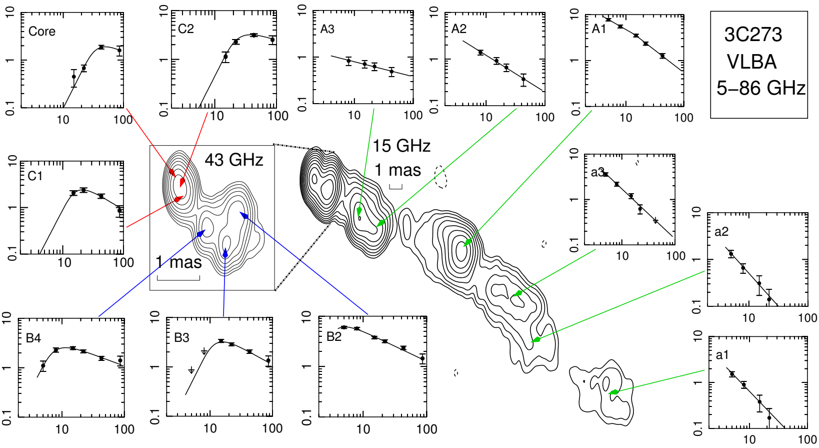

Savolainen et al. 2008

3C273 example: Spectral Decomposition of the Core Region

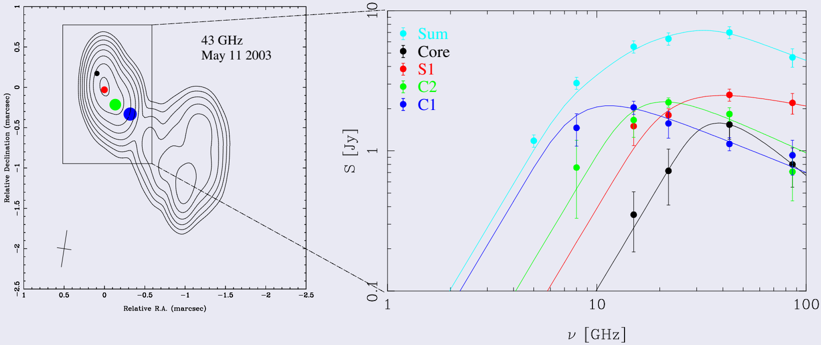

Elongated, rather flat-spectrum core can be decomposed into a series of self-absorbed synctrotron components

3C273 example: Spectral Turnover

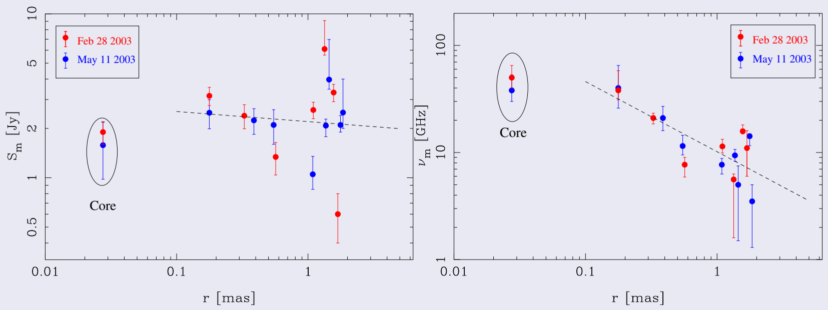

- The synchrotron peak frequency decreases as function of distance from the core: $\nu_{\rm m} \propto r^{-0.7\pm0.1}$
- Confirms the composite nature of the flat radio spectrum

3C273 example: Magnetic Flux Density

$\log(B)$ vs. $\log(r)$

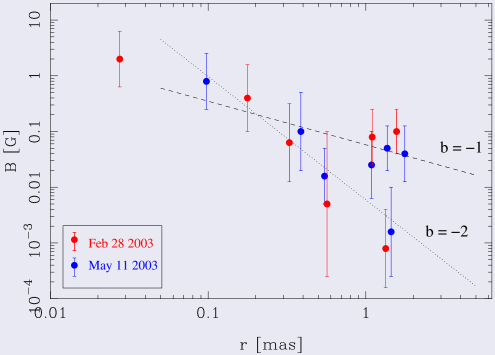

- In the core, $B \sim 1\,\mathrm{G}$
- On average $B \propto r^{-b}$ with b between 1 and 2.

3C273 example: Magnetic Flux Density

$\log(B)$ vs. $\log(r)$

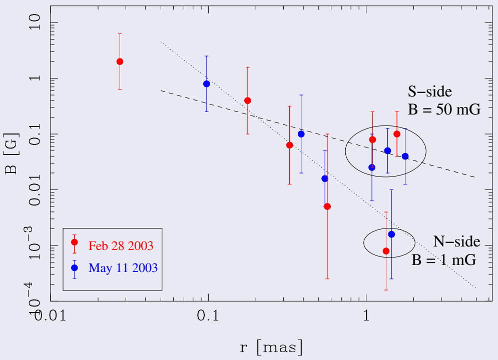

- In the core, $B \sim 1\,\mathrm{G}$
- On average $B \propto r^{-b}$ with b between 1 and 2.
- Significant B gradient across the jet at 1.5 mas from the core: Northern side $\sim 1\,\mathrm{mG}$ while Southern side $\sim 50\,\mathrm{mG}$. This may be a sign that the assumption of random B-field orientation is not valid in pc-scale jet of 3C273.

Lower limit for total energy stored in particles and fields in a synchrotron source

- Assume a homogeneous, stationary synchrotron source with volume $V = \pi L^3/6$ at a distance D_L (e.g., a giant radio lobe). Using previously derived formula: $F_\nu^{tot} = 13.5 a(p) \frac{n_0 V B^{(p+1)/2}}{D_\mathrm{L}^2} \left(\frac{6.26\times10^{18}}{\nu}\right)^{(p-1)/2}$ [Jy]

Lower limit for total energy stored in particles and fields in a synchrotron source

- Assume a homogeneous, stationary synchrotron source with volume $V = \pi L^3/6$ at a distance D_L (e.g., a giant radio lobe). Using previously derived formula: $F_\nu^{tot} = 13.5 a(p) \frac{n_0 V B^{(p+1)/2}}{D_\mathrm{L}^2} \left(\frac{6.26\times10^{18}}{\nu}\right)^{(p-1)/2}$ [Jy]
- Integrate this over frequency between the limits where spectrum is power-law. This gives the total observed flux in that frequency interval and one can solve for n_0.

Lower limit for total energy stored in particles and fields in a synchrotron source

- Assume a homogeneous, stationary synchrotron source with volume $V = \pi L^3/6$ at a distance $D_{\rm L}$ (e.g., a giant radio lobe). Using previously derived formula: $F_\nu^{tot} = 13.5 a(p) \frac{n_0 V B^{(p+1)/2}}{D_{\rm L}^2} \left(\frac{6.26\times 10^{18}}{\nu}\right)^{(p-1)/2}$ [Jy]
- Integrate this over frequency between the limits where spectrum is power-law. This gives the total observed flux in that frequency interval and one can solve for n_0.
- The total energy in relativistic electrons is then $W_e = V \int_{\gamma_1}^{\gamma_2} n_0 \gamma^{-p+1} d\gamma = f(\nu, p) \frac{D_{\rm L}^2 F(\nu)}{B^{3/2}}$.

Lower limit for total energy stored in particles and fields in a synchrotron source

- Assume a homogeneous, stationary synchrotron source with volume $V = \pi L^3/6$ at a distance D_L (e.g., a giant radio lobe). Using previously derived formula: $F_\nu^{tot} = 13.5a(p)\frac{n_0 V B^{(p+1)/2}}{D_\mathrm{L}^2}\left(\frac{6.26\times10^{18}}{\nu}\right)^{(p-1)/2}$ [Jy]
- Integrate this over frequency between the limits where spectrum is power-law. This gives the total observed flux in that frequency interval and one can solve for n_0.
- The total energy in relativistic electrons is then $W_e = V\int_{\gamma_1}^{\gamma_2} n_0\gamma^{-p+1}d\gamma = f(\nu,p)\frac{D_\mathrm{L}^2 F(\nu)}{B^{3/2}}$.
- Let k be the fraction of particle energy not in relativistic electrons or positrons. Now particle energy $W_p = (1+k)W_e$, magnetic energy is $W_B = VB^2$ and the total energy as a function of field strenght is $W_{tot} = (1+k)W_e + W_B = C_1(1+k)B^{-3/2} + C_2B^2$.

Lower limit for total energy stored in particles and fields in a synchrotron source

- Assume a homogeneous, stationary synchrotron source with volume $V = \pi L^3/6$ at a distance $D_{\rm L}$ (e.g., a giant radio lobe). Using previously derived formula: $F_\nu^{tot} = 13.5a(p)\frac{n_0 VB^{(p+1)/2}}{D_{\rm L}^2}\left(\frac{6.26\times10^{18}}{\nu}\right)^{(p-1)/2}$ [Jy]
- Integrate this over frequency between the limits where spectrum is power-law. This gives the total observed flux in that frequency interval and one can solve for n_0.
- The total energy in relativistic electrons is then $W_e = V\int_{\gamma_1}^{\gamma_2} n_0\gamma^{-p+1}d\gamma = f(\nu,p)\frac{D_{\rm L}^2 F(\nu)}{B^{3/2}}$.
- Let k be the fraction of particle energy not in relativistic electrons or positrons. Now particle energy $W_p = (1+k)W_e$, magnetic energy is $W_B = VB^2$ and the total energy as a function of field strenght is $W_{tot} = (1+k)W_e + W_B = C_1(1+k)B^{-3/2} + C_2B^2$.
- W_{tot} is minimized for $W_B = 3/4(1+k)W_e$, i.e. rough equipartition between particles and B-field.

Lower limit for W_{tot} in FR-II lobes

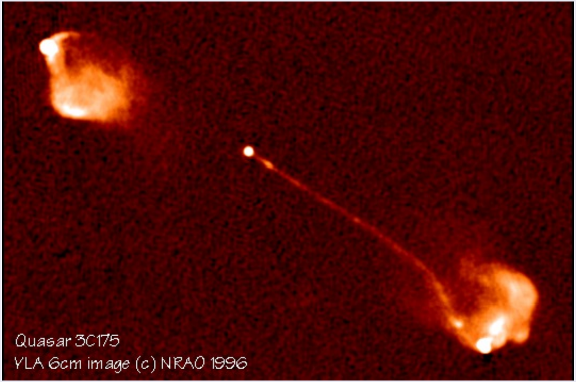

- Minimum energy stored in large FR-II radio lobes is 10^{60} ergs, but this is sensitive to k and to the volume filling factor.
- Given the filamentary structure, there is likely more energy in non-relativistic gas than in relativistic $\rightarrow W_{tot}$ could be in excess of 10^{61} ergs

Synchrotron losses and spectral breaks

- Synchrotron losses are proportional to γ^2 (as are inverse Compton losses, shown later) $\rightarrow$ highest energy electrons suffer most rapid losses
- Radiative losses shape the electron energy distribution and they have a well-defined effect on the observed radiation spectrum $\rightarrow$ if initial electron energy distribution is known, observed spectrum can be used to measure the age of the source
- Continuity equation for $n(\gamma, t)$: $\frac{\partial n(\gamma,t)}{\partial t} + \frac{\partial}{\partial \gamma}\left(n(\gamma, t)\frac{d\gamma}{dt}\right) = q(\gamma, t) - p(\gamma, t)$, where q and p are the source and sink terms, respectively and $d\gamma/dt$ includes radiative and other losses

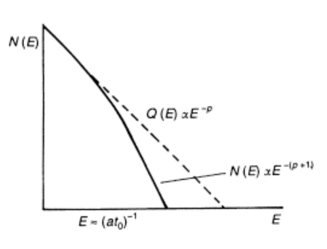

- For synchrotron losses only ($d\gamma/dt = -k\gamma^2$), the initial injected power-law electron spectrum steepens by $\Delta p = 1$, i.e., emission spectrum steepens by $\Delta\alpha = 0.5$, at energy $\gamma = 1/(kt)$

Radio galaxy ages

- Measured spectral ages for large FR-II lobes are typically $10^7 - 10^8$ yr
- Agrees with the age from the source size divided by the advance speeds of the hot spots ($\lesssim 0.1c$)

Mack et al. (1998)

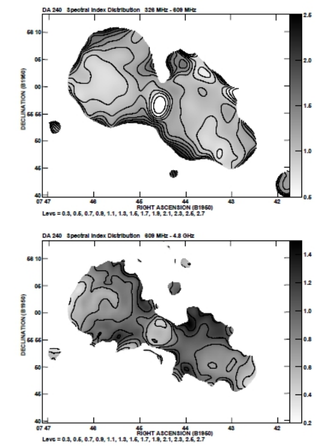

Inverse Compton scattering

Compton scattering

- Electrons can exchange energy with photons via Compton scattering (electron gains energy) and inverse Compton scattering (electron loses energy)

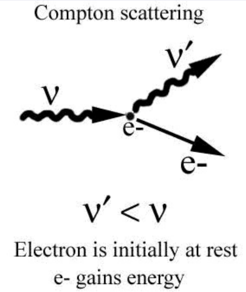

Compton scattering

- Electrons can exchange energy with photons via Compton scattering (electron gains energy) and inverse Compton scattering (electron loses energy)
- Compton scattering from an electron at rest is an inherently quantum mechanical phenomenon. Recoil of electron makes scattering inelastic, unlike in classical case, and energy transfer takes place $\epsilon_1 = \frac{\epsilon}{1+\frac{\epsilon}{mc^2}(1-\cos\theta)}$

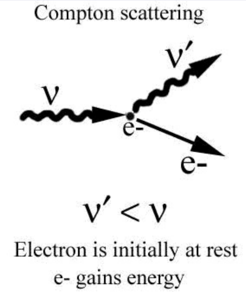

Compton scattering

- Electrons can exchange energy with photons via Compton scattering (electron gains energy) and inverse Compton scattering (electron loses energy)
- Compton scattering from an electron at rest is an inherently quantum mechanical phenomenon. Recoil of electron makes scattering inelastic, unlike in classical case, and energy transfer takes place $\epsilon_1 = \frac{\epsilon}{1+\frac{\epsilon}{mc^2}(1-\cos\theta)}$
- Quantum effects also change the scattering cross-section from Thomson cross section to *Klein-Nishina* cross-section. The main effect here is the reduction of cross-section when photon energy becomes of the order of $m_e c^2$.

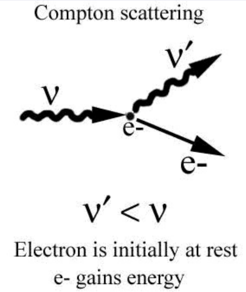

Inverse Compton scattering

- If moving electron has sufficient kinetic energy compared to the photon, net energy may be transfered from electron to photon in *inverse Compton* scattering.

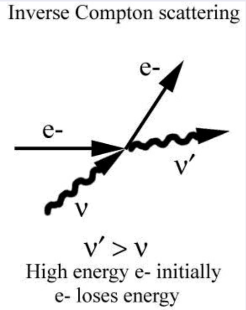

Inverse Compton scattering

- If moving electron has sufficient kinetic energy compared to the photon, net energy may be transfered from electron to photon in *inverse Compton* scattering.
- Assuming $h\nu << m_e c^2$ one can transform from the observer's frame to electron rest frame, scatter there elastically, and Lorentz transform back. Doppler shift for the photon energy seen by the electron $\epsilon' = \epsilon\gamma(1 - \beta\cos\theta)$ while the scattered photon energy seen by the observer is $\epsilon_1 = \epsilon'_1\gamma(1 + \beta\cos\theta'_1)$

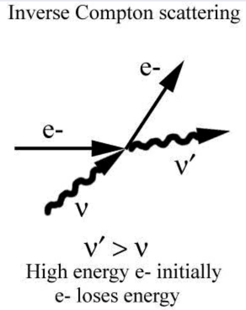

Inverse Compton scattering

- If moving electron has sufficient kinetic energy compared to the photon, net energy may be transfered from electron to photon in *inverse Compton* scattering.
- Assuming $h\nu << m_e c^2$ one can transform from the observer's frame to electron rest frame, scatter there elastically, and Lorentz transform back. Doppler shift for the photon energy seen by the electron $\epsilon' = \epsilon\gamma(1 - \beta\cos\theta)$ while the scattered photon energy seen by the observer is $\epsilon_1 = \epsilon_1'\gamma(1 + \beta\cos\theta_1')$
- For relativistic electrons, it is apparent that the energy of the scattered photon increases by $\approx \gamma^2$, since θ and θ_1' are typically $\approx \pi/2$.

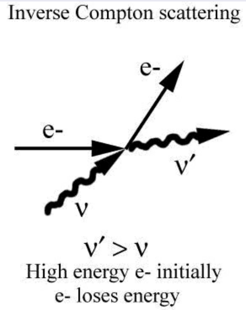

Energy losses by inverse Compton scattering

- Scattering probability, and the number of scatterings per unit time, is proportional to number density of photons n_{ph}. Combining this with previous results, gives for total scattered power $P_{IC} \propto \epsilon n_{ph} \gamma^2 \propto \gamma^2 U_{rad}$ where U_{rad} is the energy density of the radiation field.

Energy losses by inverse Compton scattering

- Scattering probability, and the number of scatterings per unit time, is proportional to number density of photons n_{ph}. Combining this with previous results, gives for total scattered power $P_{IC} \propto \epsilon n_{ph} \gamma^2 \propto \gamma^2 U_{rad}$ where U_{rad} is the energy density of the radiation field.
- The exact form for the radiated power per electron is derived in R&L Ch. 7. The end result is $P_{IC} = (4/3)\sigma_T c \gamma^2 \beta^2 U_{rad}$.

Energy losses by inverse Compton scattering

- Scattering probability, and the number of scatterings per unit time, is proportional to number density of photons n_{ph}. Combining this with previous results, gives for total scattered power $P_{IC} \propto \epsilon n_{ph} \gamma^2 \propto \gamma^2 U_{rad}$ where U_{rad} is the energy density of the radiation field.
- The exact form for the radiated power per electron is derived in R&L Ch. 7. The end result is $P_{IC} = (4/3)\sigma_T c \gamma^2 \beta^2 U_{rad}$.
- Compare this with synchrotron power derived earlier: $P_{synch} = (4/3)\sigma_T c \gamma^2 \beta^2 U_B \rightarrow \frac{P_{synch}}{P_{IC}} = \frac{U_B}{U_{rad}}$ The main cooling mechanism depends on the energy densities.

Energy losses by inverse Compton scattering

- Scattering probability, and the number of scatterings per unit time, is proportional to number density of photons n_{ph}. Combining this with previous results, gives for total scattered power $P_{IC} \propto \epsilon n_{ph} \gamma^2 \propto \gamma^2 U_{rad}$ where U_{rad} is the energy density of the radiation field.
- The exact form for the radiated power per electron is derived in R&L Ch. 7. The end result is $P_{IC} = (4/3)\sigma_T c \gamma^2 \beta^2 U_{rad}$.
- Compare this with synchrotron power derived earlier: $P_{synch} = (4/3)\sigma_T c \gamma^2 \beta^2 U_B \rightarrow \frac{P_{synch}}{P_{IC}} = \frac{U_B}{U_{rad}}$ The main cooling mechanism depends on the energy densities.
- IC spectrum from a power-law electron distribution is a power-law $\alpha_{IC} = -(p-1)/2$.

Synchrotron self-Compton

- In jets, relativistic electrons emit synchrotron photons from radio up to X-rays. The same electrons can then scatter these photons up to γ-ray energies. This is called *synchrotron self-Compton* mechanism. SSC flux increases quadratically with relativistic electron density (synchrotron flux linearly).
- In Belloni's book, Marscher gives an approximate formula for SSC flux (7.26) as a function of synchrotron peak flux, peak frequency and emission region size
- In SSC, all seed photons that can scatter up to X/γ-rays contribute equally: low-energy photons (abundant) are scattered by high energy electrons (rare), mid-energy photons scattered by mid-energy electrons, and high-energy photons (rare) scattered by low-energy electrons (abundant).
- SSC losses are difficult to calculate: depend on retarded radiation field seen by electrons at each point of the source. BUT radiation field depends on the history of electron energy distribution which depends on the history of losses...

Example: BL Lac SED

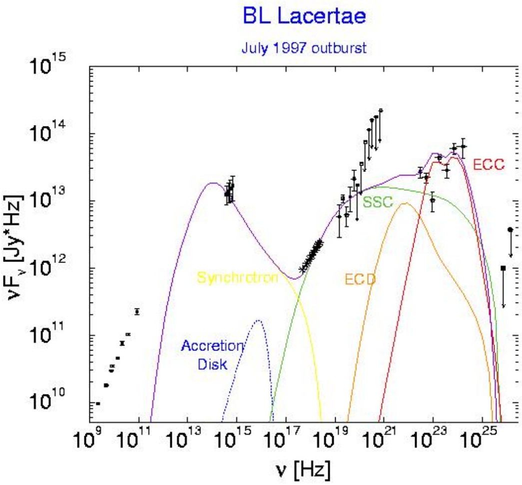

Courtesy of M. Böttcher

T_B limit due to IC catastrophe

- In a classical paper Kellermann & Pauliny-Toth (1969) pointed out that self-Compton radiation also contributes to U_{rad} and leads to significant second-order scattering as the SSC contribution to U_{rad} approaches synchrotron contribution.
- This runaway positive feedback is a very sensitive function of T_B
- IC losses cool the source very efficiently if the source rest frame T_B exceeds 10^{12} K

Pair production

Compact jets can be significant emitters of γ-rays up to TeV energies. They also have very small emission regions as deduced from variability, $R \sim 10^{12}$ cm.

Pair production

Compact jets can be significant emitters of γ-rays up to TeV energies. They also have very small emission regions as deduced from variability, $R \sim 10^{12}$ cm.

- High photon density n_γ may enable pair production $\gamma + \gamma \rightarrow e^- + e^+$, if photon energy $> m_e c^2 = 511\,\mathrm{keV}$

Pair production

Compact jets can be significant emitters of γ-rays up to TeV energies. They also have very small emission regions as deduced from variability, $R \sim 10^{12}$ cm.

- High photon density n_γ may enable pair production $\gamma + \gamma \rightarrow e^- + e^+$, if photon energy $> m_e c^2 = 511\,\mathrm{keV}$
- Optical depth for pair production $\tau_{\gamma\gamma} = n_\gamma \sigma_{\gamma\gamma} R$, where cross section $\sigma_{\gamma\gamma}$ is close to Thomson cross section near the threshold

Pair production

Compact jets can be significant emitters of γ-rays up to TeV energies. They also have very small emission regions as deduced from variability, $R \sim 10^{12}$ cm.

- High photon density n_γ may enable pair production $\gamma + \gamma \rightarrow e^- + e^+$, if photon energy $> m_e c^2 = 511\,\mathrm{keV}$
- Optical depth for pair production $\tau_{\gamma\gamma} = n_\gamma \sigma_{\gamma\gamma} R$, where cross section $\sigma_{\gamma\gamma}$ is close to Thomson cross section near the threshold
- $n_\gamma \sim \frac{L_\gamma}{4\pi R^2 m_e c^3}$ and therefore $\tau_{\gamma\gamma} \sim 200 \left(\frac{L_\gamma}{10^{48}\mathrm{ergs}^{-1}}\right)\left(\frac{10^{12}\mathrm{cm}}{R}\right)$, i.e., photons cannot escape unless relativistic effects decrease the inferred rest-frame photon density

Pair production

Compact jets can be significant emitters of γ-rays up to TeV energies. They also have very small emission regions as deduced from variability, $R \sim 10^{12}$ cm.

- High photon density n_γ may enable pair production $\gamma + \gamma \rightarrow e^- + e^+$, if photon energy $> m_e c^2 = 511\,\mathrm{keV}$
- Optical depth for pair production $\tau_{\gamma\gamma} = n_\gamma \sigma_{\gamma\gamma} R$, where cross section $\sigma_{\gamma\gamma}$ is close to Thomson cross section near the threshold
- $n_\gamma \sim \frac{L_\gamma}{4\pi R^2 m_e c^3}$ and therefore $\tau_{\gamma\gamma} \sim 200 \left(\frac{L_\gamma}{10^{48}\mathrm{ergs}^{-1}}\right)\left(\frac{10^{12}\mathrm{cm}}{R}\right)$, i.e., photons cannot escape unless relativistic effects decrease the inferred rest-frame photon density
- Highly luminous γ-ray emission with short time scale of variability provides an independent proof of relativistic motion in compact jets.